Phosphoinositide 3-Kinase γ Regulates Airway Smooth Muscle Contraction by Modulating Calcium Oscillations

Haihong Jiang, Peter W. Abel, Myron L. Toews, Caishu Deng, Thomas B. Casale, Yan Xie, and Yaping Tu

Departments of Pharmacology (H.J., P.W.A., Y.X., Y.T.), Internal Medicine (T.B.C.), and Pathology (C.D.), Creighton University School of Medicine, Omaha, Nebraska; and Department of Pharmacology and Experimental Neuroscience, University of Nebraska Medical Center, Omaha, Nebraska (M.L.T.)

ABSTRACT

Phosphoinositide 3-kinase γ (PI3Kγ) has been implicated in the pathogenesis of asthma, but its mechanism has been considered indirect, through release of inflammatory cell mediators. Because airway smooth muscle (ASM) contractile hyper-responsiveness plays a critical role in asthma, the aim of the present study was to determine whether PI3Kγ can directly regulate contractility of ASM. Immunohistochemistry staining indicated expression of PI3Kγ protein in ASM cells of mouse trachea and lung, which was confirmed by Western blot analysis in isolated mouse tracheal ASM cells. PI3Kγ inhibitor II inhibited acetylcholine (ACh)-stimulated airway contraction of cultured precision-cut mouse lung slices in a dose-dependent manner with 75% inhibition at 10 μM. In contrast, inhibitors of PI3Kα, PI3Kβ, or PI3Kδ, at concentrations 40-fold higher than their reported IC_{50} values for their primary targets, had no effect. It is noteworthy that airways in lung slices pretreated with PI3Kγ inhibitor II still exhibited an ACh-induced initial contraction, but the sustained contraction was significantly reduced. Furthermore, the PI3Kγ-selective inhibitor had a small inhibitory effect on the ACh-stimulated initial Ca^{2+} transient in ASM cells of mouse lung slices or isolated mouse ASM cells but significantly attenuated the sustained Ca^{2+} oscillations that are critical for sustained airway contraction. This report is the first to show that PI3Kγ directly controls contractility of airways through regulation of Ca^{2+} oscillations in ASM cells. Thus, in addition to effects on airway inflammation, PI3Kγ inhibitors may also exert direct effects on the airway contraction that contribute to pathologic airway hyper-responsiveness.

Introduction

Asthma ranks within the top 10 most prevalent conditions causing limitation of activity and affects approximately 23 million Americans (Morosco and Kiley, 2007). Although airway hyper-responsiveness (AHR), an exaggerated narrowing of airways induced by airway smooth muscle (ASM) cell contraction, is one of the main pathophysiologic hallmarks of asthma (Janssen and Killian, 2006; Solway and Irvin, 2007), the precise mechanisms promoting excessive contraction of ASM cells in this disease is poorly understood.

Phosphoinositide 3-kinases (PI3Ks) are known to play a prominent role in fundamental cellular responses of various cells. Previous studies using two broad spectrum inhibitors of PI3K—wortmannin and 2-(4-morpholinyl)-8-(4-aminophenyl)-4H-1-benzopyrone-4-one (LY294002)—suggested that PI3K contributes to the pathogenesis of asthma by affecting the recruitment, activation, and apoptosis of inflammatory cells (Ezeamuzie et al., 2001; Kwak et al., 2003). The class I PI3K family is divided into class IA (PI3Kα, PI3Kβ, and PI3Kδ isoforms) and class IB (the PI3Kγ isoform only). Recent reports showed that allergen-induced eosinophilic airway inflammation, AHR, and airway remodeling were all reduced in PI3Kγ knockout mice (Lim et al., 2009; Takeda et al., 2009). In a murine asthma model, aerosolized 3-[2,4-diamino-6-(3-hydroxyphenyl)pteridin-7-yl]phenol (TG100-115), an inhibitor of PI3Kγ and PI3Kδ, markedly reduced asthmatic symptoms,

including both the pulmonary eosinophilia and the AHR (Doukas et al., 2009). These studies suggest that PI3Kγ may be a novel therapeutic target in asthma and other respiratory diseases, such as chronic obstructive pulmonary disease (Marwick et al., 2010). Because PI3Kγ has a restricted distribution, primarily in cells of the hematopoietic lineage, effects of PI3Kγ inhibitors or gene knockout have been largely attributed to regulation of inflammatory responses. Although AHR can be associated with airway inflammation, the critical effect that directly leads to airway narrowing is contraction of ASM cells (An et al., 2007). Whether PI3Kγ is directly involved in hypercontractility of ASM in asthma is unknown.

It is generally accepted that binding of the neurotransmitter acetylcholine (ACh) to muscarinic receptors, which are G protein-coupled receptors (GPCRs), leads to an initial Ca^{2+} transient that is associated with a rapid contraction of ASM (Shieh et al., 1991; Bergner and Sanderson, 2002). This initial Ca^{2+} transient is followed by Ca^{2+} oscillations that trigger a sustained ASM contraction (Roux et al., 1997). It is noteworthy that PI3Kγ is only activated by various GPCRs, whereas PI3Kα, PI3Kβ, and PI3Kδ are typically stimulated by receptor tyrosine kinases (Leopoldt et al., 1998; Vanhaesebroeck and Waterfield, 1999). However, the possible role of PI3Kγ in muscarinic receptor-dependent Ca^{2+} signaling events in ASM cells has not been addressed previously.

The purpose of the present study was to determine whether PI3Kγ is directly involved in regulating ACh-induced Ca^{2+} signaling and contraction of ASM. We used both whole airways in mouse lung slices and isolated mouse ASM cells as models. We found that PI3Kγ protein is expressed in ASM cells and that PI3Kγ inhibitor II, but not inhibitors of other PI3K isoforms, can inhibit ACh-stimulated contraction of ASM cells. More importantly, our data indicate that blockade of PI3Kγ selectively suppresses ACh-induced Ca^{2+} oscillations in ASM cells, and thus attenuates ACh-induced sustained airway contraction, a key contributor to the AHR associated with asthma.

Materials and Methods

Reagents. Hanks' balanced salt solution (HBSS) supplemented with 10 mM HEPES buffer, penicillin, streptomycin, amphotericin B, Fluo-4/AM, Fura-2/AM, Pluronic F-127, Alexa Fluor 488-labeled anti-rabbit IgG, and Alexa Fluor 594-labeled anti-mouse IgG were obtained from Invitrogen (Carlsbad, CA). LY294002, N-((1E)-(6-bromoimidazo-[1,2-a]pyridin-3-yl)methylene)-N'-methyl-N''-(2-methyl-5-nitrobenzene)sulfonohydrazide, HCl (PI3Kα inhibitor VIII), 7-methyl-2-(morpholin-4-yl)-9-(1-phenylaminoethyl)-pyrido[1,2-a]-pyrimidin-4-one (PI3Kβ inhibitor VI), and 5-(2,2-difluoro-benzo[1,3]dioxol-5-ylmethylene)-thiazolidine-2,4-dione (PI3Kγ inhibitor II) were purchased from EMD Biosciences (San Diego, CA). PI3Kδ inhibitor 2-(6-aminopurin-9-ylmethyl)-3-(2-chlorophenyl)-6,7-dimethoxy-3H-quinazoli-n-4-one (IC87114) was obtained from Symansis (Washdyke, New Zealand). Rabbit PI3Kγ antibody and IRDye800-labeled anti-rabbit IgG were purchased from Cell Signaling Technology Inc. (Danvers, MA) and LI-COR Bioscience (Lincoln, NE), respectively. ACh and anti-smooth muscle α-actin antibody were purchased from Sigma-Aldrich (St. Louis, MO). Unless indicated otherwise, other reagents were purchased from either Sigma-Aldrich or Thermo Fisher Scientific (Waltham, MA). C57BL/6J mice used in our study were gifts from Dr. Stephen J. Gold (University of Texas Southwestern Medical Center, Dallas, TX). All the experiments

were approved by the Creighton University Institutional Animal Care and Use Committee.

Preparation of Lung Slices. Lung slices were prepared as described previously (Bergner and Sanderson, 2002; Bergner et al., 2006). In brief, C57BL/6J mice (15–18 weeks old) were euthanized by CO_2 followed by cervical dislocation. The lungs were inflated with 1.5 ml of 2.0% agarose-HBSS at 37°C. To stiffen the soft lung tissue for sectioning, the agarose was gelled by placing the mouse at 4°C. The lungs were then removed, and slices of 150-μm thickness were cut with an EMS-4000 tissue slicer (Electron Microscopy Sciences, Fort Washington, PA). The slices were maintained by floating them in serum-free Dulbecco's modified Eagle's medium containing antibiotics (100 U/ml penicillin and 100 μg/ml streptomycin) and antimycotic (amphotericin B, 1.5 μg/ml) at 37°C in 5% CO_2 for up to 3 days.

Measurement of Airway Contraction. Lung slices with airways that were free of agarose and completely lined by epithelial cells with beating cilia were selected for study. The slices were placed on glass coverslips in a self-constructed chamber, held in position by a piece of nylon mesh (Small Parts, Inc., Miami Lakes, FL), and visualized with a Nikon (Melville, NY) TE200 inverted microscope using a 20× objective. The bathing solution for all the experiments was HBSS with 10 mM HEPES buffer. Phase-contrast images were recorded with a digital CoolSNAP HQ2 camera (Photometrics, Tucson, AZ) using Image-Pro Plus software (MediaCybernetics, Inc., Bethesda, MD). Frames were captured in time-lapse mode (1 frame/ 3 s), and time-dependent changes in the cross-sectional areas of the airway lumen were measured by pixel summing using Image-Pro Plus. A decrease in the cross-sectional area was considered to be airway contraction.

Isolation and Culture of Tracheal ASM Cells. Cell isolation and culture were as described previously (Wong et al., 1998; Tollet et al., 2002). In brief, C57BL/6J mice were euthanized by CO_2 followed by cervical dislocation. Trachea were removed and transferred into ice-cold Krebs' solution (110.9 mM NaCl, 5.9 mM KCl, 1.1 mM $MgCl_2$, 2 mM $CaCl_2$, 1.2 mM NaH_2PO_4, 25 mM $NaHCO_3$, and 9.6 mM glucose, pH 7.4) containing antibiotics and antimycotic. Connective tissue and airway epithelium were removed by firmly scraping the luminal surface. The trachea strips were cut into small pieces (approximately 1 mm^3) and cultured in smooth muscle cell growth medium from Genlantis (San Diego, CA) containing antibiotics and antimycotic at 37°C in 5% CO_2. ASM cells began to migrate out of the fragments after 1 week. The cells were dissociated with 0.05% trypsin and subcultured in smooth muscle cell growth medium. Mouse tracheal ASM cells below passage 5 were used in all the experiments.

Measurement of Contraction of Isolated ASM Cells. ASM cells were sparsely plated onto glass coverslips and cultured overnight. The coverslips were mounted in a custom-made Plexiglas (Altuglas International, Arkema Inc., Philadelphia, PA) chamber, and images were taken using an inverted Nikon TE200 microscope equipped with a CoolSNAP HQ2 digital camera (Photometrics). An initial recording (time = 0 min) was made to obtain the size of quiescent cells. ACh (10 μM) was added to the chamber at 30 s, and images were recorded at 10-s intervals for 5 min. Contractility was assessed as described previously (Govindaraju et al., 2006). In brief, the images were digitized, and the surface area of individual cells was analyzed using Image-Pro Plus (MediaCybernetics, Inc.). Only those cells with a distinct longitudinal axis and clearly visible cell-substrate boundaries were selected for analysis. Surface area was obtained by tracing the outer boundary of the cell. Three experiments were performed with 50 cells recorded in each experiment. The extent of contraction was calculated as the ratio of the change in surface area to the initial value.

Immunohistochemistry. Lungs and trachea were removed and fixed with buffered formalin for immunohistochemistry staining of PI3Kγ. In brief, formalin-fixed tissues were paraffin-embedded, and 5-μm-thick sections were prepared, deparaffinized in xylene, and hydrated through a graded alcohol series. Rabbit PI3Kγ antibody and biotin-conjugated goat anti-rabbit IgG from Vector Laboratories

(Burlingame, CA) were used as the primary antibody and secondary antibody, respectively. The negative control used nonimmune rabbit IgG as the primary antibody. Standard methods were then used for hematoxylin and eosin staining of tissues.

Immunofluorescence Microscopy. ASM cells grown on glass coverslips were fixed with methanol and acetone (1:1) for 10 min. PI3Kγ and α-actin were visualized by rabbit anti-PI3Kγ antibody and mouse anti-α-actin antibody followed by Alexa Fluor 488-labeled anti-rabbit IgG and/or Alexa Fluor 594-labeled anti-mouse IgG, respectively. Images were captured by CoolSNAP CF camera (Photometrics) attached to a Nikon Ti-80 microscope.

Measurement of Ca²⁺ Signaling in Single ASM Cells of Lung Slices. Lung slices were loaded with 10 μM Fluo-4/AM in HBSS containing 0.02% Pluronic F-127 (Invitrogen) and 100 μM sulfobromophthalein (to inhibit efflux of de-esterified Fluo-4) for 1 h at 37°C. This was followed by incubation for 30 min at room temperature in HBSS containing 100 μM sulfobromophthalein to allow for the de-esterification of Fluo-4/AM (Bergner et al., 2006). Lung slices were mounted in a perfusion chamber, and fluorescence images of live lung slices were acquired at 2 frames/s by an LSM 510 META NLO confocal microscope (Creighton University Integrated Biomedical Imaging Facility) using a 488-nm laser and a 500- to 530-nm band pass filter. Fluorescence intensity (F), indicative of intracellular Ca²⁺, was measured in selected regions of interest (3 × 3 pixels) in individual ASM cells and was expressed as fluorescence ratio (F/F$_0$) after normalizing to the fluorescence intensity immediately before the addition of ACh (F$_0$) as described previously (Bergner et al., 2006). Data shown are the averages from at least 20 cells.

Measurement of Intracellular Free Ca²⁺ in Isolated ASM Cells. Glass coverslips with cultured ASM cells were incubated for 1 h at 37°C in HBSS/1% bovine serum albumin buffer containing Fura-2/AM (4 μM), 0.02% Pluronic F-127 (Invitrogen), and 100 μM sulfobromophthalein. The Fura-2-loaded cells were washed twice with HBSS and then incubated in the dark at room temperature for 30 min. Cells were then excited at 340 and 380 nm using a DeltaRAM X monochronometer (Photon Technology International, Inc., Birmingham, NJ). Fluorescent images of individual cells were acquired at 1 frame/s for at least 300 s to characterize Ca²⁺ transients and Ca²⁺ oscillations after ACh stimulation. The intracellular free calcium concentration in selected regions of interest (3 × 3 pixels) of individual cells is presented as the ratio of the fluorescence intensities (500-nm emission) at excitation of 340 nm compared with 380 nm (Xie et al., 2009). Data are averages from at least 25 cells.

Ca²⁺ Oscillation Frequency. There were at least six data points within each oscillation. Oscillation amplitude was defined as the difference between the peak and the proceeding basal level of fluorescence. Background noise was determined as the oscillations of fluorescence signal acquired before ACh stimulation. A fluorescence signal was defined as a Ca²⁺ oscillation only if the peak amplitude was greater than twice the background noise. Ca²⁺ oscillation frequency was measured as the inverse of the average time between two oscillations.

Protein Extraction, Electrophoresis, and Western Blot Analysis. Protein was extracted from homogenized mouse lungs, hearts, and exponentially growing ASM cells using 1× radioimmunoprecipitation assay complete lysis buffer (Santa Cruz Biotechnology, Inc., Santa Cruz, CA). Protein concentrations were determined using the Bradford assay (Bio-Rad Laboratories, Hercules, CA). Protein samples (60 μg) were loaded on 8% SDS polyacrylamide gels, electrophoresed, and transferred onto a polyvinylidene difluoride membrane. Membranes were blocked using blocking buffer for 1 h at room temperature. The membranes were then probed with a PI3Kγ-specific antibody followed by IRDye800-labeled anti-rabbit IgG. β-Actin was used as a loading control. The signal was visualized using an Odyssey IR imaging system (LI-COR Bioscience).

Data Analysis. Data are expressed as means ± S.E. Groups were compared using a Student's *t* test for unpaired observations. A probability level (*p*) of 0.05 was used to determine statistical significance.

Results

Expression of PI3Kγ in Mouse Airways. Immunohistochemical analysis of PI3Kγ protein expression in mouse trachea and lung was performed (Fig. 1A). PI3Kγ immunoreactivity was observed in ASM and airway epithelium of mouse trachea (Fig. 1Aa) and lung tissues (Fig. 1Ac) stained with the PI3Kγ-specific antibody but not in tissues stained with control rabbit IgG (Fig. 1A, b and d). Tracheal cartilage was negative for PI3Kγ staining (Fig. 1Aa).

Western blot analysis confirmed expression of PI3Kγ protein in mouse lung. PI3Kγ protein was also detected in mouse heart, which was used as a positive control (Patrucco et al., 2004). In addition, PI3Kγ was expressed in isolated mouse ASM cells in culture (Fig. 1B). This result was confirmed by immunofluorescence staining of isolated mouse ASM cells with PI3Kγ-specific antibody (Fig. 1C). As a control, these ASM cells show positive staining for α-actin, a marker of smooth muscle cells.

Blockade of PI3Kγ Attenuates ACh-Induced Airway Contraction in Cultured Precision-Cut Mouse Lung Slices. To determine which PI3K isoform(s) can regulate
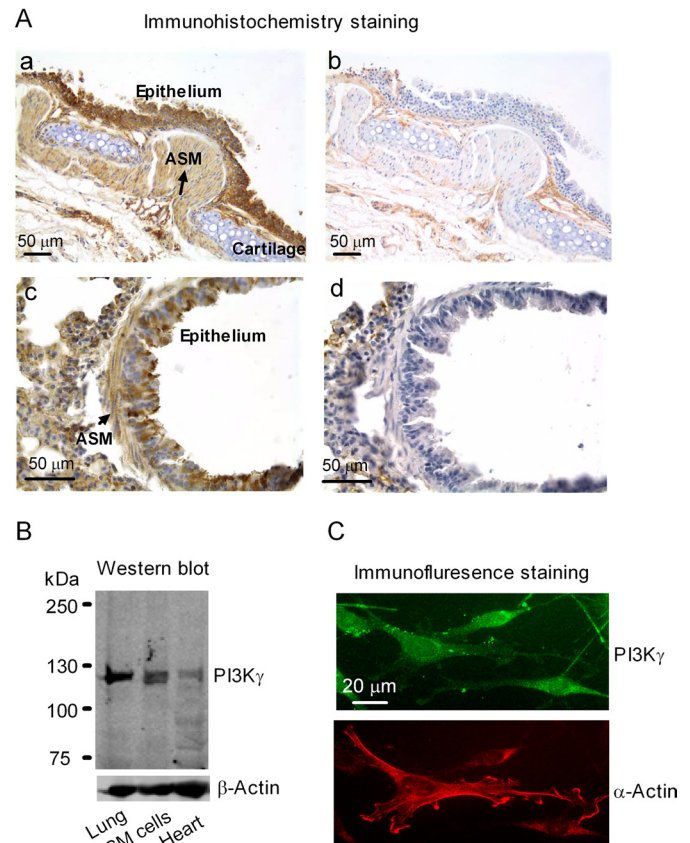

Fig. 1. Expression of PI3Kγ protein in mouse ASM cells. A, representative immunohistochemical staining of PI3Kγ protein in mouse trachea (a) and lung slices (c) using a PI3Kγ-specific antibody or isotype-specific negative control antibody (rabbit IgG) in a parallel section of trachea (b) and lung slices (d). PI3Kγ staining was localized in ASM and epithelium but not in cartilage. All the sections were counterstained with blue hematoxylin. B, Western blot analysis of PI3Kγ protein in lysates of mouse lung tissue, heart tissue, and isolated mouse ASM cells using a PI3Kγ-specific antibody. Images shown are representative of four independent experiments. β-Actin was used as a loading control. C, immunofluorescent staining of PI3Kγ protein (green) in cultured mouse ASM cells, and staining of α-actin (red) as a marker of smooth muscle cells.
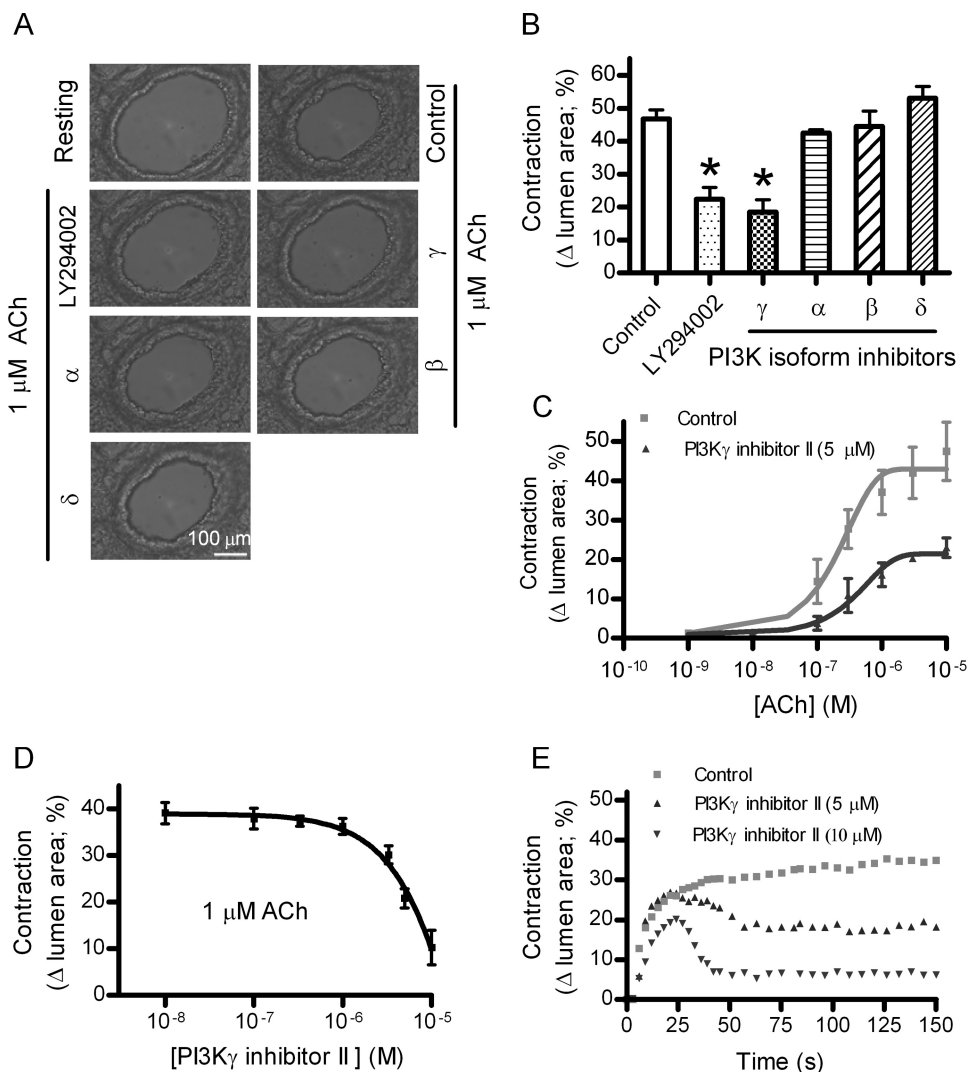
A

B

C

Fig. 2. Blockade of PI3Kγ inhibits airway contractility of airways in mouse lung slices in response to ACh. Lung slices were pretreated without (control) or with PI3K isoform-selective inhibitors for 10 min before treatment with ACh to induce airway contraction. Relaxation of the airways between exposure to inhibitors and ACh was achieved by washing with buffer for 20 min. Changes in cross-sectional area of the airway lumen were monitored with phase-contrast microscopy and recorded in time-lapse mode at 1 frame/3 s. A, representative images of the airway before (resting) or after stimulation with 1 μM ACh for 10 min in the absence (control) or presence of LY294002 (10 μM), PI3Kα inhibitor (10 nM), PI3Kβ inhibitor (200 nM), PI3Kγ inhibitor II (5 μM), or PI3Kδ inhibitor (10 μM). B, the cross-sectional area of the lumen was calculated with Image-Pro Plus software (Media-Cybernetics, Inc.) to quantify contraction. Data represent the mean ± S.E., with $*$, $p < 0.01$ compared with untreated control. The data were generated in eight lung slices from four mice. C, concentration-response curves of ACh-induced airway contraction of lung slices without (control) or with pretreatment using PI3Kγ inhibitor II (5 μM). D and E, dose-dependent inhibition (D) and time-dependent inhibition (E) of 1 μM ACh-induced airway contraction of mouse lung slices by PI3Kγ inhibitor II. Each point in C and D represents mean ± S.E. using 10 lung slices from at least four different mice. Data shown in E are representative of at least 10 separate experiments.

D

E

ACh-mediated airway contraction, cultured lung slices were pretreated without or with PI3K isoform inhibitors 10 min before ACh stimulation. Airways with similar cross-sectional areas, which averaged $61,551 \pm 1341$ μm^2, were used for all the studies. Figure 2A shows an airway that was incubated without (resting) or with 1 μM ACh. ACh induced an initial phasic contraction that then stabilized at approximately 50% reduction in airway lumen cross-sectional area in the continued presence of ACh (control). Pretreatment of lung slices with 10 μM LY294002, an inhibitor of all the PI3K isoforms, reduced ACh-stimulated contraction of lung slices by $53 \pm 7\%$ (Fig. 2A, data quantified in Fig. 2B). It is noteworthy that 5 μM PI3Kγ inhibitor II (Camps et al., 2005) inhibited ACh-stimulated airway contraction by $60 \pm 8\%$, suggesting that the PI3Kγ isoform regulates contraction. Consistent with this result, inhibitors of PI3Kα, PI3Kβ, or PI3Kδ at concentrations 40-fold higher than their IC_{50} values reported for their primary targets (Sadhu et al., 2003; Jackson et al., 2005; Knight et al., 2006) had little effect (Fig. 2, A and B).

Lung slices in the absence or presence of 5 μM PI3Kγ inhibitor II were exposed to different concentrations of ACh for 10 min, and airway contraction was quantified as the change in cross-sectional area of the airway lumen. ACh

caused a concentration-dependent contraction of the airways, with a maximum decrease of $47 \pm 7\%$ in lumen area and an EC_{50} of 0.32 ± 0.04 μM (Fig. 2C). Pretreatment of lung slices with PI3Kγ inhibitor II significantly decreased the ACh-induced maximum contraction of airways by approximately half, to $23 \pm 4\%$, with no effect on the EC_{50} for ACh (control = 0.32 ± 0.04 μM; PI3Kγ inhibitor II = 0.41 ± 0.05 μM). PI3Kγ inhibitor II attenuated 1 μM ACh-induced airway contraction in a concentration-dependent manner, with 50% inhibition at 5 μM and 75% inhibition at 10 μM (Fig. 2D). It is noteworthy that airways from lung slices pretreated with PI3Kγ inhibitor II (5 or 10 μM) still exhibited the initial ACh-induced contraction but failed to maintain a sustained contraction (Fig. 2E), suggesting that PI3Kγ may be important for the sustained phase of ACh-induced airway contraction.

PI3Kγ Regulates ACh-Induced Ca^{2+} Oscillations of ASM Cells in Lung Slices. Ca^{2+} is the key signaling molecule for ASM contraction. Therefore, Ca^{2+} signaling of single ASM cells within lung slices was assessed by two-photon microscopy (Fig. 3). After addition of 10 μM ACh, a rapid initial increase in intracellular Ca^{2+} occurred (Fig. 3, A and B), followed by sustained Ca^{2+} oscillations (Fig. 3B). Pretreatment of lung slices with PI3Kγ inhibitor II (5 μM) had a
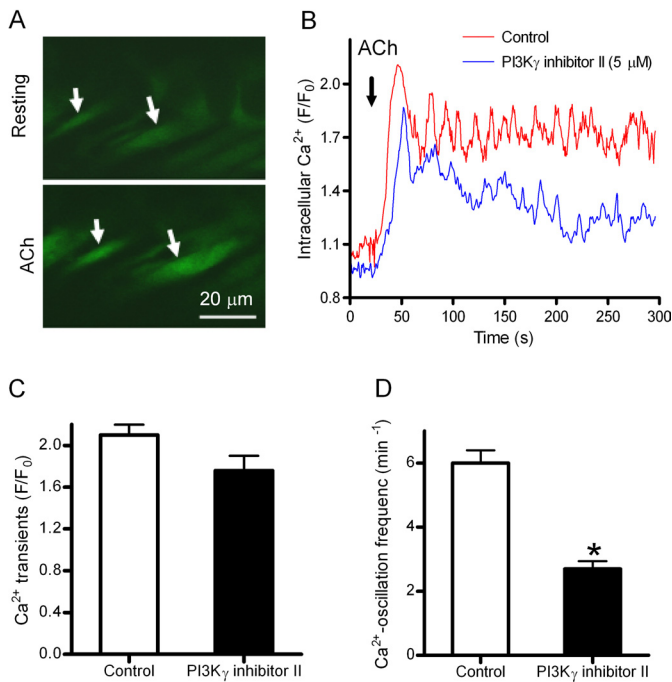
Fig. 3. Blockade of PI3Kγ selectively attenuates Ca^{2+} oscillations in ASM cells in lung slices. The ACh-induced increase in intracellular $[Ca^{2+}]_i$ in single ASM cells of lung slices loaded with Ca^{2+} indicator dye Fluo-4-AM was assessed using confocal microscopy. A, ASM cells (arrow) in the airway wall. This representative image shows the ASM immediately before and 15 s after the addition of 1 μM ACh. B, representative traces of ACh-induced Ca^{2+} signaling in ASM cells of lung slices in the absence (control) or presence of PI3Kγ inhibitor II (5 μM). Fluorescence intensity (F) was expressed as fluorescence ratio (F/F_0) after normalizing to the fluorescence intensity immediately before the addition of ACh (F_0). C, no significant effects of PI3Kγ inhibitor II on the ACh-induced initial Ca^{2+} transient. D, inhibition of the frequency of ACh-induced Ca^{2+} oscillations by PI3Kγ inhibitor II. Values in C and D are means ± S.E. from at least 20 ASM cells in airways of different lung slices from four mice with ∗, $p <$ 0.01 compared with control cells.

small inhibitory effect on the initial Ca^{2+} transient (Fig. 3B, quantified in Fig. 3C) but substantially attenuated the sustained phase of Ca^{2+} signaling (Fig. 3B), thus making ACh-stimulated Ca^{2+} signaling more transient. More importantly, PI3Kγ inhibitor II reduced the frequency of ACh-induced Ca^{2+} oscillations during the sustained phase by approximately 55% (Fig. 3B, quantified in Fig. 3D).

PI3Kγ Regulates ACh-Induced Intracellular Ca^{2+} Mobilization and Contraction of Isolated ASM Cells. The effects of PI3Kγ inhibitor II on Ca^{2+} signaling was also assessed in isolated mouse ASM cells. ACh (10 μM) induced a marked increase in intracellular Ca^{2+} (Fig. 4A). This response consisted of an initial Ca^{2+} transient followed by Ca^{2+} oscillations. PI3Kγ inhibitor II (5 μM) again had a small inhibitory effect on the initial ACh-induced Ca^{2+} transient, but it made ACh-stimulated Ca^{2+} signaling more transient and significantly reduced the frequency of ACh-induced Ca^{2+} oscillations by 39% (Fig. 4A, quantified in Fig. 4, B and C).

The effects of PI3Kγ inhibitor II on contraction of isolated ASM cells were also assessed. Treatment of cells with 10 μM ACh for 5 min caused contraction of ASM cells (Fig. 4D), with a marked reduction in the area of individual ASM cells by 33.6 ± 4.2% compared with cells in the absence of ACh (Fig. 4E). In contrast, 10 μM ACh reduced the area of individual ASM cells pretreated with 5 μM PI3Kγ inhibitor II by only

13.3 ± 2.4% (Fig. 4E), a 60% inhibition of the ACh-induced contraction.

Discussion

Only a few studies have examined expression and functions of PI3Kγ in nonhematopoietic cell types. PI3Kγ is abundant in sympathetic neurons and plays an important role in signal transduction pathways necessary for cell survival (May et al., 2010). PI3Kγ also plays a key role in cardiovascular homeostasis (reviewed by Hawkins and Stephens, 2007). For example, activation of PI3Kγ in cardiac myocytes regulates Ca^{2+} oscillations, thus modulating cardiac autonomic activity (Bony et al., 2001). PI3Kγ also regulates myocyte contractility (Patrucco et al., 2004) and angiotensin II-mediated contraction of vascular smooth muscle (Vecchione et al., 2005). However, the expression and functions of PI3Kγ in ASM have not been investigated.

In the present study, we used cultured precision-cut mouse lung slices and isolated mouse ASM cells to test for PI3Kγ effects. We showed that PI3Kγ protein is expressed in ASM cells and that a PI3Kγ-selective inhibitor, but not inhibitors of other class I PI3K isoforms, inhibited both ACh-stimulated Ca^{2+} signaling and contraction of airways and isolated ASM cells. Our study is the first to show that PI3Kγ can regulate airway contraction by controlling GPCR-stimulated intracellular Ca^{2+} signaling in ASM cells. Because excessive contraction of ASM cells is a key component of the AHR that is a primary pathophysiologic characteristic of asthma, our data suggest that targeting PI3Kγ in ASM cells may be an important approach to reduce AHR and treat airway contraction in asthma.

Previous studies have linked PI3Kγ with asthma (Lim et al., 2009; Takeda et al., 2009), and an inhibitor of PI3Kγ markedly reduced asthmatic symptoms in a murine asthma model (Doukas et al., 2009). However, those studies focused on the role of PI3Kγ in the eosinophil-mediated airway inflammation component of asthma. Although airway contraction may be increased by airway inflammation, airway narrowing is most-directly controlled by contraction of ASM cells. However, whether PI3Kγ has direct effects on ASM contractility was not investigated. Because our immunohistochemical staining, Western blot analysis, and immunofluorescence staining all showed the expression of PI3Kγ protein in ASM cells of mouse trachea and lung, we investigated whether selective pharmacological attenuation of PI3Kγ activity in ASM cells would affect GPCR-stimulated airway contraction.

Using cultured precision-cut mouse lung slices, we found that PI3Kγ inhibitor II inhibited ACh-induced airway contraction in a concentration-dependent manner, whereas inhibitors of PI3Kα, PI3Kβ, or PI3Kδ at concentrations 40-fold higher than their IC_{50} values reported for their primary targets had little or no effect on contraction. These data suggest that PI3Kγ, but not PI3Kα, PI3Kβ, or PI3Kδ, is an important regulator of ACh-induced contraction of airways. This was also supported by our data showing that 10 μM LY294002, a broad-spectrum PI3K inhibitor with a much higher IC_{50} for PI3Kγ (7.3 μM) compared with other PI3K isoforms (Smith et al., 2007), inhibited ACh-induced airway contraction by only 50%.
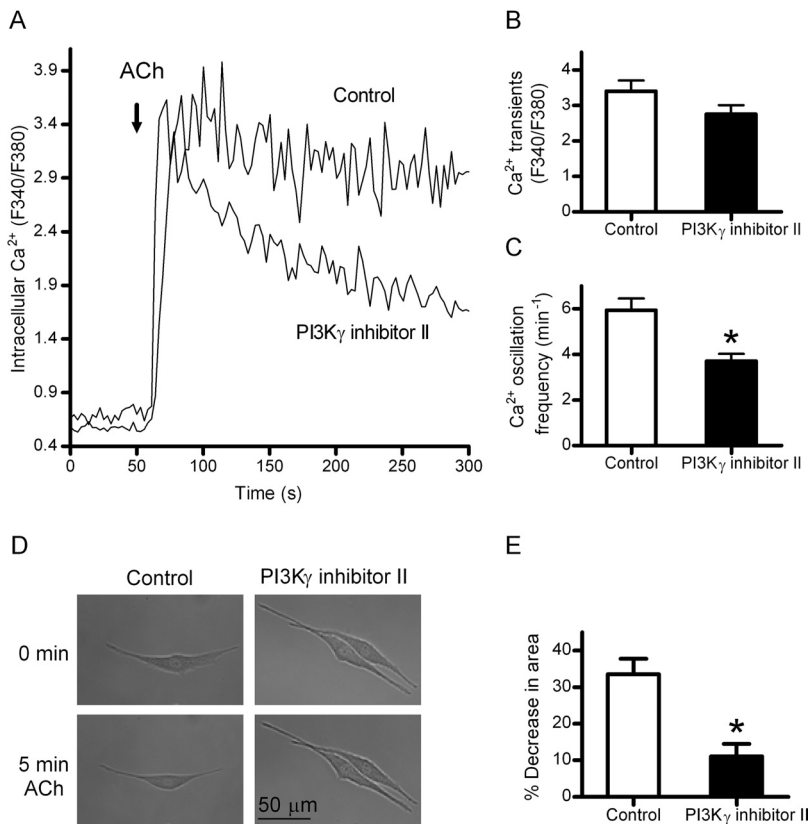
Further analysis of PI3Kγ inhibition on the time course of

Fig. 4. Blockade of PI3Kγ attenuates ACh-induced intracellular Ca^{2+} signaling and contraction of isolated mouse ASM cells. A through C, cells were preloaded with Ca^{2+} indicator dye Fura-2/AM. A, representative traces of intracellular Ca^{2+} in response to 10 μM ACh in the absence (control) and presence of PI3Kγ inhibitor II (5 μM). The intracellular free calcium concentration is presented as the ratio of the fluorescence intensities at excitation of 340 nm compared with 380 nm (F340/F380). B, no significant effects of PI3Kγ inhibitor II on ACh-induced initial Ca^{2+} transient. C, inhibition of ACh-induced Ca^{2+} oscillations by PI3Kγ inhibitor II. D and E, blocking PI3Kγ attenuates ACh-induced contraction of ASM cells. Cultured ASM cells were exposed to 10 μM ACh in the absence (control) or presence of PI3Kγ inhibitor II (5 μM). D shows representative images of an initial recording (time = 0 min) and 5-min exposure to 10 μM ACh. The extent of contraction, calculated as the percentage change in cell surface area, is shown in E. Data shown in B, C, and E are expressed as mean ± S.E. and represent at least 25 cells from at least four separate experiments performed on multiple days with ∗, $p < 0.01$ compared with control cells.

ACh-induced airway contraction revealed that airways from lung slices pretreated with PI3Kγ inhibitor II retained a strong initial contraction, similar to that in the absence of PI3Kγ inhibitor II. In contrast, the sustained phase of contraction was substantially reduced by PI3Kγ inhibitor II. Previous studies have suggested that the biphasic ACh-induced contraction in airways is the result of parallel biphasic changes in intracellular Ca^{2+} concentrations in ASM cells (Bergner and Sanderson, 2002). Indeed, our data are consistent with previous studies showing that the ACh-induced increase in intracellular Ca^{2+} consisted of an initial Ca^{2+} transient that is responsible for initial contraction, followed by Ca^{2+} oscillations that are critical for maintenance of sustained airway contraction (Roux et al., 1997). As expected from our contraction data, PI3Kγ inhibitor II only slightly reduced the initial Ca^{2+} transient but more substantially reduced the magnitude of the sustained phase of Ca^{2+} signaling in ASM cells in lung slices, thus making ACh-stimulated Ca^{2+} signaling more transient. The frequency of the ACh-induced Ca^{2+} oscillations was also reduced by PI3Kγ inhibitor II, and both the decreased magnitude and frequency of the Ca^{2+} changes probably contribute to its selective inhibitory effect on sustained airway contraction.

To directly test this hypothesis, we isolated ASM cells from mouse trachea and examined the effects of PI3Kγ inhibitor II on ACh-induced Ca^{2+} signaling and contraction of isolated ASM cells. ACh caused a marked reduction in isolated ASM cell area, indicative of cell contraction. In contrast, ASM cells pretreated with PI3Kγ inhibitor II exhibited significantly smaller reductions of cell area in response to ACh stimulation. Similar to results with intact lung slices, PI3Kγ inhibitor II showed a marked inhibition in both the magnitude of the sustained Ca^{2+} increase and in the frequency of Ca^{2+}

oscillations of isolated ASM cells. Together these results suggest that PI3Kγ may be involved in the sustained phase of ASM contraction by regulating the sustained phase of Ca^{2+} increases and oscillations. It is noteworthy that PI3Kγ has been reported to play a role in regulation of both cardiac muscle and vascular smooth muscle contraction (Patrucco et al., 2004; Vecchione et al., 2005). Thus, it is possible that PI3Kγ regulation of airway smooth muscle contraction by controlling Ca^{2+} oscillations may well be a more general regulatory mechanism for this enzyme.

Additional details of the molecular mechanisms underlying PI3Kγ-dependent regulation of Ca^{2+} signaling in ASM cells remain to be established. ACh causes airway constriction by activating smooth muscle muscarinic ACh receptors, a GPCR that conveys signals by dissociating inactive G proteins into active Gα and Gβγ subunits. In ASM cells, it is generally accepted that activation of the G$_q$-coupled muscarinic receptor by ACh leads to the G$_q$α-dependent phospholipase C activation, causing oscillatory Ca^{2+} signal that generates ASM tone. However, it is now clear that Gβγ also plays prominent roles in signal transduction through its numerous downstream effectors (Sternweis, 1994; Smrcka, 2008; Kirui et al., 2010). Because PI3Kγ is known to be selectively activated by Gβγ subunits rather than Gα subunits (Leopoldt et al., 1998), our data suggest that Gβγ-dependent PI3Kγ activation may be involved in ACh-induced Ca^{2+} oscillations and contraction of ASM cells.

In summary, our data show that PI3Kγ is expressed in ASM cells and plays an important role in the sustained phase of airway contraction by regulating GPCR-stimulated Ca^{2+} oscillations in ASM cells. Understanding the GPCR/PI3Kγ/Ca^{2+} signaling pathway in ASM may provide additional pharmacological targets for development of new drugs to

ameliorate AHR in asthma and other airway diseases characterized by airway obstruction.

References

An SS, Bai TR, Bates JH, Black JL, Brown RH, Brusasco V, Chitano P, Deng L, Dowell M, Eidelman DH, et al. (2007) Airway smooth muscle dynamics: a common pathway of airway obstruction in asthma. *Eur Respir J* **29:**834–860.

Bergner A and Sanderson MJ (2002) Acetylcholine-induced calcium signaling and contraction of airway smooth muscle cells in lung slices. *J Gen Physiol* **119:**187–198.

Bergner A, Kellner J, Silva AK, Gamarra F, and Huber RM (2006) Ca^{2+}-signaling in airway smooth muscle cells is altered in T-bet knock-out mice. *Respir Res* **7:**33.

Bony C, Roche S, Shuichi U, Sasaki T, Crackower MA, Penninger J, Mano H, and Pucéat M (2001) A specific role of phosphatidylinositol 3-kinase gamma. A regulation of autonomic Ca(2)+ oscillations in cardiac cells. *J Cell Biol* **152:**717–728.

Camps M, Rückle T, Ji H, Ardissone V, Rintelen F, Shaw J, Ferrandi C, Chabert C, Gillieron C, Françon B, et al. (2005) Blockade of PI3Kgamma suppresses joint inflammation and damage in mouse models of rheumatoid arthritis. *Nat Med* **11:**936–943.

Doukas J, Eide L, Stebbins K, Racanelli-Layton A, Dellamary L, Martin M, Dneprovskaia E, Noronha G, Soll R, Wrasidlo W, et al. (2009) Aerosolized phosphoinositide 3-kinase γ/δ inhibitor TG100–115 [3-[2,4-diamino-6-(3-hydroxyphenyl)pteridin-7-yl]phenol] as a therapeutic candidate for asthma and chronic obstructive pulmonary disease. *J Pharmacol Exp Ther* **328:**758–765.

Ezeamuzie CI, Sukumaran J, and Philips E (2001) Effect of wortmannin on human eosinophil responses in vitro and on bronchial inflammation and airway hyperresponsiveness in Guinea pigs in vivo. *Am J Respir Crit Care Med* **164:**1633–1639.

Govindaraju V, Michoud MC, Al-Chalabi M, Ferraro P, Powell WS, and Martin JG (2006) Interleukin-8: novel roles in human airway smooth muscle cell contraction and migration. *Am J Physiol Cell Physiol* **291:**C957–C965.

Hawkins PT and Stephens LR (2007) PI3Kγ is a key regulator of inflammatory responses and cardiovascular homeostasis. *Science* **318:**64–66.

Jackson SP, Schoenwaelder SM, Goncalves I, Nesbitt WS, Yap CL, Wright CE, Kenche V, Anderson KE, Dopheide SM, Yuan Y, et al. (2005) PI 3-kinase p110β: a new target for antithrombotic therapy. *Nat Med* **11:**507–514.

Janssen LJ and Killian K (2006) Airway smooth muscle as a target of asthma therapy: history and new directions. *Respir Res* **7:**123.

Kirui JK, Xie Y, Wolff DW, Jiang H, Abel PW, and Tu Y (2010) Gβγ signaling promotes breast cancer cell migration and invasion. *J Pharmacol Exp Ther* **333:**393–403.

Knight ZA, Gonzalez B, Feldman ME, Zunder ER, Goldenberg DD, Williams O, Loewith R, Stokoe D, Balla A, Toth B, et al. (2006) A pharmacological map of the PI3-K family defines a role for p110alpha in insulin signaling. *Cell* **125:**733–747.

Kwak YG, Song CH, Yi HK, Hwang PH, Kim JS, Lee KS, and Lee YC (2003) Involvement of PTEN in airway hyperresponsiveness and inflammation in bronchial asthma. *J Clin Invest* **111:**1083–1092.

Leopoldt D, Hanck T, Exner T, Maier U, Wetzker R, and Nürnberg B (1998) Gβγ stimulates phosphoinositide 3-kinase-gamma by direct interaction with two domains of the catalytic p110 subunit. *J Biol Chem* **273:**7024–7029.

Lim DH, Cho JY, Song DJ, Lee SY, Miller M, and Broide DH (2009) PI3Kγ-deficient mice have reduced levels of allergen-induced eosinophilic inflammation and airway remodeling. *Am J Physiol Lung Cell Mol Physiol* **296:**L210–L219.

Marwick JA, Chung KF, and Adcock IM (2010) Phosphatidylinositol 3-kinase isoforms as targets in respiratory disease. *Ther Adv Respir Dis.* **4:**19–34.

May V, Lutz E, MacKenzie C, Schutz KC, Dozark K, and Braas KM (2010) Pituitary adenylate cyclase activating polypeptide (PACAP)/PAC1HOP1 receptor activation coordinates multiple neurotrophic signaling pathways: Akt activation through phosphatidylinositol 3-kinase gamma and vesicle endocytosis for neuronal survival. *J Biol Chem* **285:**9749–9761.

Morosco G and Kiley J (2007) Expert Panel Report 3 (EPR-3): guidelines for the diagnosis and management of asthma- summary report 2007. *J Allergy Clin Immunol* **120 (Suppl):**s93–s138.

Patrucco E, Notte A, Barberis L, Selvetella G, Maffei A, Brancaccio M, Marengo S, Russo G, Azzolino O, Rybalkin SD, et al. (2004) PI3Kgamma modulates the cardiac response to chronic pressure overload by distinct kinase-dependent and -independent effects. *Cell* **118:**375–387.

Roux E, Guibert C, Savineau JP, and Marthan R (1997) $[Ca^{2+}]i$ oscillations induced by muscarinic stimulation in airway smooth muscle cells: receptor subtypes and correlation with the mechanical activity. *Br J Pharmacol* **120:**1294–1301.

Sadhu C, Masinovsky B, Dick K, Sowell CG, and Staunton DE (2003) Essential role of phosphoinositide 3-kinase delta in neutrophil directional movement. *J Immunol* **170:**2647–2654.

Shieh CC, Petrini MF, Dwyer TM, and Farley JM (1991) Concentration-dependence of acetylcholine-induced changes in calcium and tension in swine trachealis. *J Pharmacol Exp Ther* **256:**141–148.

Smith LD, Hickman ES, Parry RV, Westwick J, and Ward SG (2007) PI3Kγ is the dominant isoform involved in migratory responses of human T lymphocytes: effects of ex vivo maintenance and limitations of non-viral delivery of siRNA. *Cell Signal* **19:**2528–2539.

Smrcka AV (2008) G protein betagamma subunits: central mediators of G protein-coupled receptor signaling. *Cell Mol Life Sci* **65:**2191–2214.

Solway J and Irvin CG (2007) Airway smooth muscle as a target for asthma therapy. *N Engl J Med* **356:**1367–1369.

Sternweis PC (1994) The active role of beta gamma in signal transduction. *Curr Opin Cell Biol* **6:**198–203.

Takeda M, Ito W, Tanabe M, Ueki S, Kato H, Kihara J, Tanigai T, Chiba T, Yamaguchi K, Kayaba H, et al. (2009) Allergic airway hyperresponsiveness, inflammation, and remodeling do not develop in phosphoinositide 3-kinase γ-deficient mice. *J Allergy Clin Immunol* **123:**805–812.

Tollet J, Everett AW, and Sparrow MP (2002) Development of neural tissue and airway smooth muscle in fetal mouse lung explants: a role for glial-derived neurotrophic factor in lung innervation. *Am J Respir Cell Mol Biol* **26:**420–429.

Vanhaesebroeck B and Waterfield MD (1999) Signaling by distinct classes of phosphoinositide 3-kinases. *Exp Cell Res* **253:**239–254.

Vecchione C, Patrucco E, Marino G, Barberis L, Poulet R, Aretini A, Maffei A, Gentile MT, Storto M, Azzolino O, et al. (2005) Protection from angiotensin II-mediated vasculotoxic and hypertensive response in mice lacking PI3Kgamma. *J Exp Med* **201:**1217–1228.

Wong JZ, Woodcock-Mitchell J, Mitchell J, Rippetoe P, White S, Absher M, Baldor L, Evans J, McHugh KM, and Low RB (1998) Smooth muscle actin and myosin expression in cultured airway smooth muscle cells. *Am J Physiol* **274:**L786–L792.

Xie Y, Wolff DW, Wei T, Wang B, Deng C, Kirui JK, Jiang H, Qin J, Abel PW, and Tu Y (2009) Breast cancer migration and invasion depend on proteasome degradation of regulator of G-protein signaling 4. *Cancer Res* **69:**5743–5751.

Address correspondence to: Yaping Tu, Creighton University School of Medicine, Department of Pharmacology, 2500 California Plaza, Omaha, NE 68178. E-mail: yapingtu@creighton.edu